Impacts of Operating Hardware on Window Thermal Performance

Robert Hart[1], Cezary Misiopecki[2], Arild Gustavsen[3], Bjørn Petter Jelle[4], Dariush Arasteh[5]

ABSTRACT

Windows are responsible for about 40 percent of the heat loss through typical building envelopes so lowering window frame and glazing unit U-factors will reduce the impact of windows on the energy use in buildings. The thermal effects of operating hardware are currently ignored in the relatively low performing double pane windows common today, but may become significant in high performance windows. This paper describes simulation studies analyzing thermal-bridging effects of non-continuous operating (and non-operating) hardware in common casement style window frame designs. We use finite volume computational fluid dynamics modeling to demonstrate the change in frame sill profile U-factor for configurations using typical hardware systems.

Some conclusions can be drawn regarding the impacts of operating hardware on the thermal performance based on the individual frames profiles, although few general trends can be observed due to the large design differences between each frame section modeled in this study. Two of the three out-opening casement profiles modeled show reduced performance greater than 0.05 W/(m^2 K), which may be significant when carried to whole windows in National Fenestration Rating Council (NFRC) and International Organization for Standardization (ISO) rating systems. Fastener types, hardware location within the frame, and other factors related to the method of hardware implementation may significantly impact the effect of hardware on the frame. Neither the base performance level nor the primary frame material appears to determine the thermal effect of hardware based on those metrics alone.

INTRODUCTION

Minimizing thermal transmittance (U-factor) of building envelopes through the optimization of materials and components is a key energy-efficiency strategy. Windows are responsible for about 40 percent of the heat loss through typical building envelopes so lowering window frame and glazing unit U-factors will reduce the impact of windows on the energy use in buildings.

The most insulating glazing units currently have U-factors as low as 0.3-0.5 Watts per square meter Kelvin (W/(m^2 K)) and typically employ three glass layers, two or more low-emissivity (low-e) coatings, and an inert gas fill. The most insulating window frames have U-factors as low as 0.6 - 0.8 W/(m^2 K) and typically employ low thermal conductivity materials within, or part of, the structural frame (Gustavsen et al. 2007, Jelle et al. 2012).

Previous work described simulation studies analyzing the effects of frame and spacer surface emissivity and conductivity. That work defined research targets for window frame components that will result in better frame thermal performance than is exhibited

[1]Robert Hart, Scientific Engineering Associate, Lawrence Berkeley National Laboratory, Berkeley, California, USA
[2]Cezary Misiopecki, Ph.D. Candidate, Norwegian University of Science and Technology, Trondheim, Norway
[3]Arild Gustavsen, Professor, Norwegian University of Science and Technology, Trondheim, Norway
[4]Bjørn Petter Jelle, Professor, SINTEF Building and Infrastructure / Norwegian University of Science and Technology, Trondheim, Norway
[5]Dariush Arasteh, Research Scientist, Lawrence Berkeley National Laboratory, Berkeley, California, USA

by the best products available on the market today (Gustavsen et al. 2011).

This paper expands on the previous work by describing simulation studies analyzing thermal bridging effects of non-continuous operating (and non-operating) hardware in common casement style window frame designs. We use finite volume computational fluid dynamics (CFD) modeling to demonstrate the change in sill U-factor for configurations using typical hardware systems. The thermal effects of hardware are currently ignored in the relatively low performing double pane windows common today, but may become significant in high performance windows.

WINDOW FRAMES

We performed thermal performance simulations on four different window frames: One aluminum clad wood frame (Frame A), one fiberglass (Frame B), and two polyvinyl chloride (PVC) frames (Frames C and D). All the frames were of the outward-opening casement type except Frame D, which was inward opening.

The most significant hardware penetration in each frame is at the sill, therefore the sill frame cross-section is the focus of this paper. The modeled sill length of 610 mm the hardware case reflects National Fenestration Rating Council (NFRC) 100 requirements (2010). Three-dimensional frame slices 25.4 mm wide were modeled without hardware to determine the base (reference) performance. Since there are no three-dimensional effects, these models are equivalent to two-dimensional modeling.

The simulated models are simplified representations of common industry frames. Simplification significantly reduces computing time and improves numerical accuracy in the three-dimensional hardware case, but with the risk of inaccurate representation of the actual frame. To address this, we modeled both the actual design and a simplified version for each frame without hardware and verified that the simulated U-factor of the simplified models were within five percent of models with no simplifications.

To aid comparisons between the frames, the conductivity of the glazing systems is held constant. The conductivity and emissivity of all frame materials detailed in Figures 1 through 4 are listed in Tables 1 and 2.

Window Frame A

Frame A is solid wood with a thin layer of painted aluminum cladding on the exterior surface, as shown in the cross-section in Figure 1. Frame height is 71.4 mm; sightline from top of frame to bottom of glazing is 11.3 mm; and glazing width is 21.6 mm.

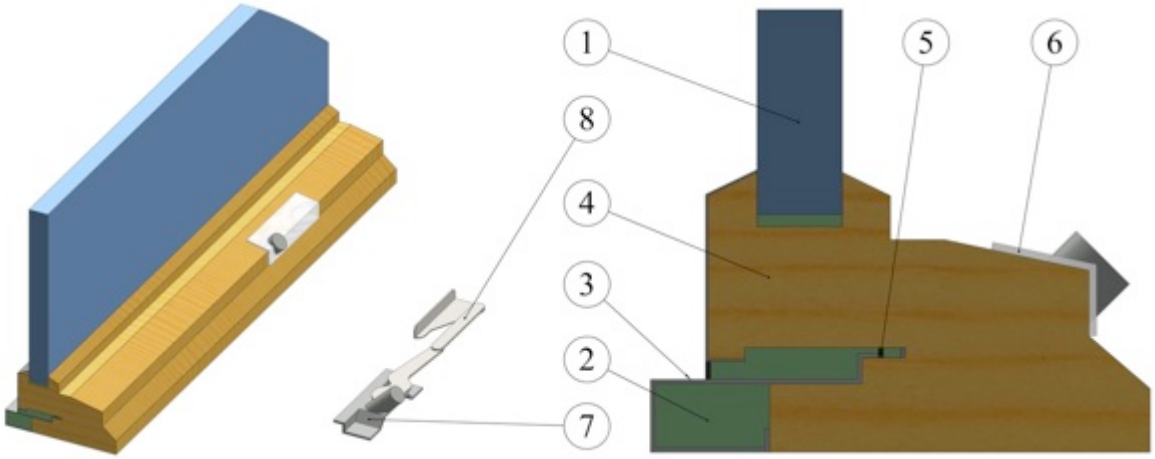

FIGURE 1. Cross-section and isometric view of Frame A and hardware

Window Frame B

Frame B is pultruded fiberglass reinforced polyethylene, as shown in the cross-section in Figure 2. Frame height is 60.8 mm; sightline from top of frame to bottom of glazing is 13.1 mm; and glazing width is 22.3 mm.

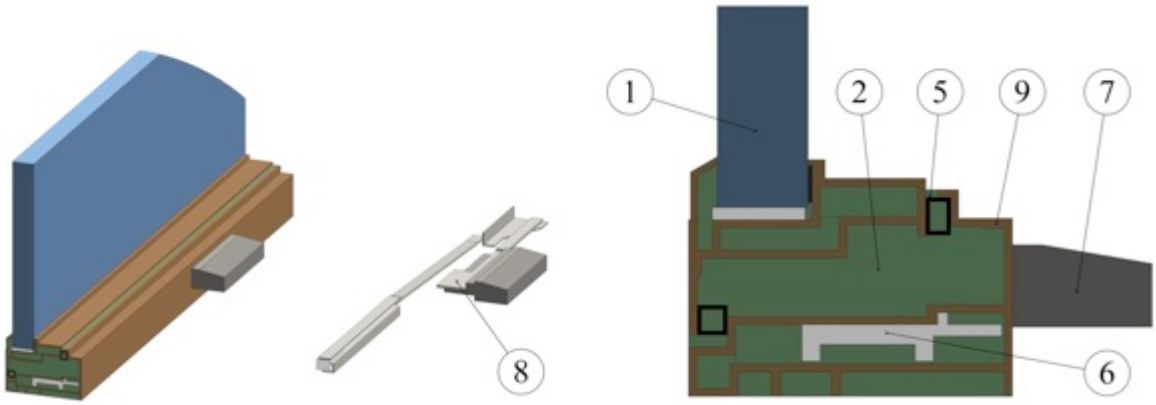

FIGURE 2. Cross-section and isometric view of Frame B and hardware

Window Frame C

Frame C is rigid polyvinylchloride (PVC), as shown in the cross-section in Figure 3. Frame height is 85.7 mm; sightline from top of frame to bottom of glazing is 12.7 mm; and glazing width is 18.9 mm.

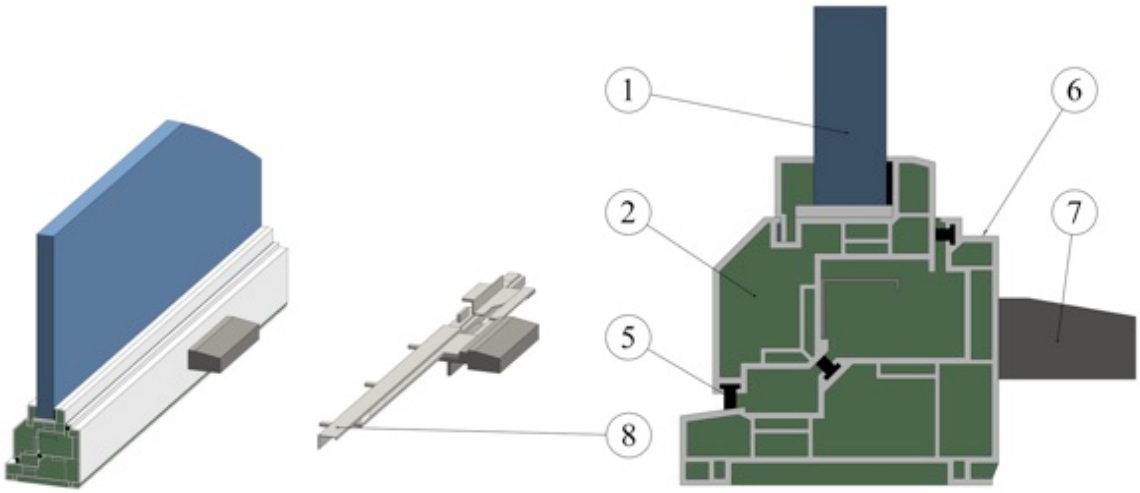

FIGURE 3. Cross-section and isometric view of Frame C and hardware

Window Frame D

Frame D is rigid PVC, as shown in the cross-section in Figure 4. Frame height is 117.0 mm; sightline from top of frame to bottom of glazing is 34.6 mm; and glazing width is 30.6 mm.

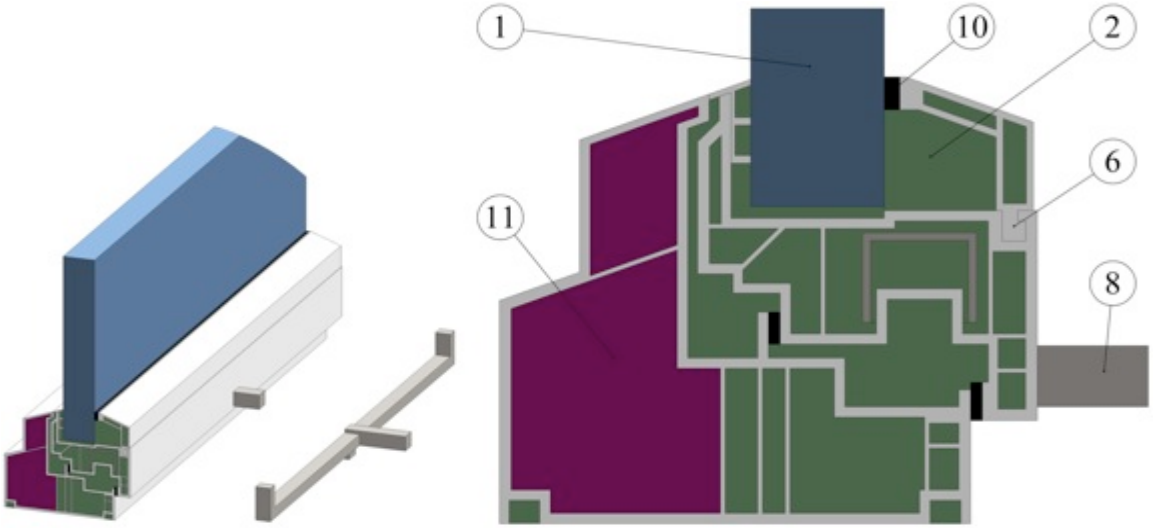

FIGURE 4. Cross-section and isometric view of Frame C and hardware

NUMERICAL PROCEDURES

In the CFD program (ANSYS Fluent Release 13) a control-volume method is used to solve the coupled heat and fluid-flow equations in three dimensions. Conduction, convection, and radiation are simulated numerically. Solid Works 2011 was used to create the window frame model and ANSYS Meshing was used as a pre-processor to create the mesh and to construct the computational domains.

The sill cross-sections were simulated in three dimensions. Three dimensions are necessary to account for the non-continuous hardware shapes in the frame members. The maximum Rayleigh number found for the frame cavities is about 1.5×10^4. The frame cavities have vertical-to-horizontal (Lv/Lh) aspect ratios lower than about five. For such Rayleigh numbers and aspect ratios, Zhao (1998) reports steady laminar flow. Although most of the cavities presented are not rectangular, incompressible and steady laminar flow is assumed in this work. Further, viscous dissipation is not addressed, and all thermophysical properties are assumed to be constant except for the buoyancy term of the y-momentum equation where the Boussinesq approximation is used. The Semi-Implicit Method for Pressure-linked Equations Consistent (SIMPLEC) was used to model the interaction between pressure and velocity. The energy and momentum variables at cell faces were found by using the Quadratic Upstream Interpolation for Convective Kinetics (QUICK) scheme. The CFD program uses central differences to approximate diffusion terms and relies on the PREssure STaggering Option scheme (PRESTO) to find the pressure values at the cell faces. Convergence was determined by checking the residuals for energy and ensuring that they were lower than 1×10^{-13}.

Radiation heat transfer was included in the simulations through use of the Surface to Surface (S2S) radiation model, which calculate the energy exchange between surfaces taking into account their size, separation distance and orientation using a geometric function called “view factor”. The S2S model ignores absorption, emission and scattering phenomena in the air cavities. The internal cavity walls were assumed to be diffuse gray. Prior to the final simulations, some grid sensitivity tests were performed on Frame D. Grid sizes of 0.5, 1, 1.5, 2, 3 and 4 mm were tested. The frame U-factors only change by 0.32% from the finest to the coarsest mesh. Because it was determined that this difference in grid size was not significant, grid sizes less than or equal to 1 mm were used in the final simulations for all of the frames. In the former studies the Discrete Transfer Radiation Model (DTRM) was used for determining radiation heat transfer within the air gaps. These simulations have also been verified experimentally (Gustavsen et al. 2001, 2010). For Frame D the U-factors were compared using the DTRM and S2S model. Differences of 0.6% and 0.04% were found respectively for DTRM with 4 rays and DTRM with 140 rays, while calculation time was significantly shorter for the S2S model.

Material Properties and Boundary Conditions

Tables 1 and 2 display the initial material properties used in the numerical simulations. Material data were obtained, if available, from NFRC 101 (2010).

TABLE 1. Conductivity and emissivity of frame materials

Number	Material	Conductivity (W/(m K))	Emissivity (-)
1	Glazing	0.0035	0.84
2	Frame air cavity	Varies	-
3	Aluminum alloys (painted)	160.0	0.8
4	Coniferous woods (softwoods)	0.140	0.9
5	EPDM seals	0.250	0.9

6	PVC - rigid	0.170	0.9
7	Zinc Cast (painted)	125.0	0.9
8	Steel (rolled, ground)	50.0	0.6
9	Fiberglass	0.300	0.9
10	Neoprene	0.230	0.9
11	Basotec foam	0.035	0.9

TABLE 2. Air properties for interior frame cavities used in CFD simulations

Property	**Value**	**Units**
Average air temperature	10.0	°C
Thermal conductivity	0.02482	W/(m K)
Specific heat capacity	1005.5	J/(kg K)
Dynamic viscosity	1.7724×10^{-5}	kg/(m s)
Density	1.2467	kg/m^3
Expansion coefficient	3.5317×10^{-3}	1/K
Gravitational acceleration	9.81	m/s^2

Simplified International Organization for Standardization (ISO) 10077-2 (2003) boundary conditions as shown in Table 3, were used in the CFD simulations. The surface heat transfer coefficients combine for a total surface heat transfer resistance of 0.17 (m^2 K)/W. The exterior and interior side boundary condition uses a fixed convection coefficient.

TABLE 3. Boundary conditions used in the simulations

Boundary Condition	**Value**	**Units**
Indoor temperature	293.15	K
Outdoor temperature	273.15	K
Density of heat flow rate of incident solar radiation on surface	0	W/m^2
Combined convection and radiation surface coefficient of heat transfer for the indoor frame and vision sections	7.692	$W/(m^2 K)$
Combined convection and radiation surface coefficient of heat transfer for the outdoor frame and vision section	25.0	$W/(m^2 K)$
Density of heat flow rate at the frame/wall interface	0	W/m^2
Density of heat flow rate at the top of center-of-glass	0	W/m^2

RESULTS AND DISCUSSION

A summary of U-factor change in each sill cross-section associated with the addition of operating hardware is shown in Table 4. Since the overall performance of each frame varies significantly, i.e. by a factor of 3.8 from Frame A to Frame D, the percent change in U-factor due to hardware cannot be used to compare the hardware effects between the units. Instead, the absolute change in U-factor provides a better gauge of hardware impact. Frames A and C show an impact of more than 0.05 W/(m^2 K), which may be significant if considered with regard to the NFRC 100 (2010) or ISO 10077-2 (2003) standards. No trends can be observed based on frame or hardware type since each frame in this study is significantly different in design. The impacts of hardware on each individual frame though are examined in depth in the following sections. Frame D shows the smallest hardware impact with respect to absolute change in the U-factor, due primarily to shallow penetration of the hardware into the frame. The absolute U-factor change due to hardware in Frame C, which has the largest hardware impact, is about 30 times that of frame D. The significant hardware impact can be attributed to multiple penetrations into the frame's cellular frame cavities.

TABLE 4. Summary of frame U-factor change with operating hardware

Frame	U-factor - Base (W/(m^2 K))	U-factor - Hardware (W/(m^2 K))	Absolute Change (W/(m^2 K))	Percent Change (%)
A	2.104	2.208	0.104	4.9
B	1.661	1.683	0.022	1.3
C	1.313	1.547	0.234	17.8
D	0.558	0.566	0.008	1.4

The hardware impact is most noticeable at the hardware penetrations through the interior frame surface. Figure 5 shows the temperature distribution along the interior surface of each frame. The coldest temperatures displayed for each frame, up to 7.2 K below the interior air temperature, are on the hardware. The lowest surface temperature of the group is on Frame A at 285.8 K, which is 1.2 K below the no hardware case. The highest surface temperature change when hardware is implemented is on Frame D at 290.5 K, which is 2.7 K below the no hardware case. This temperature reduction reduces the effective condensation resistance of the frames.

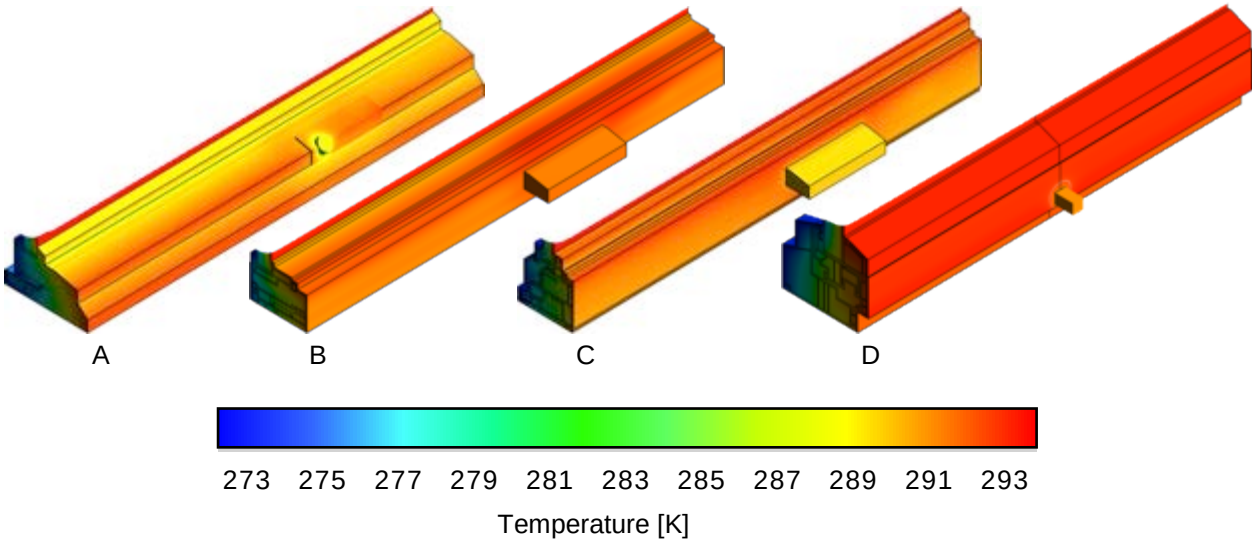

FIGURE 5. Temperature distribution along interior surface of each tested frame

Frame A

The basic wood structure in Frame A has the lowest conductivity of all frame materials investigated in this study, but the frame configuration and area of the wood in this frame results in the highest overall frame U-factor. Interior frame cavities are created in Frame A to install the internally mounted hardware. The large contact surface area and penetration depth of the hardware in these cavities combine to result in a 4.9% increase in U-factor for the hardware version of the frame. Figure 6 shows the isotherms of the frame at key cross-sections. These sections include the base frame (1), hardware (2), and frame cavity (3) cross-sections. Frame sections 1 and 3 show that the air cavity instated for hardware clearance has little impact on frame performance. The significant penetration depth and contact area of the operating hardware (2) results in high conduction and low temperatures at the hardware penetration through the interior frame surface.

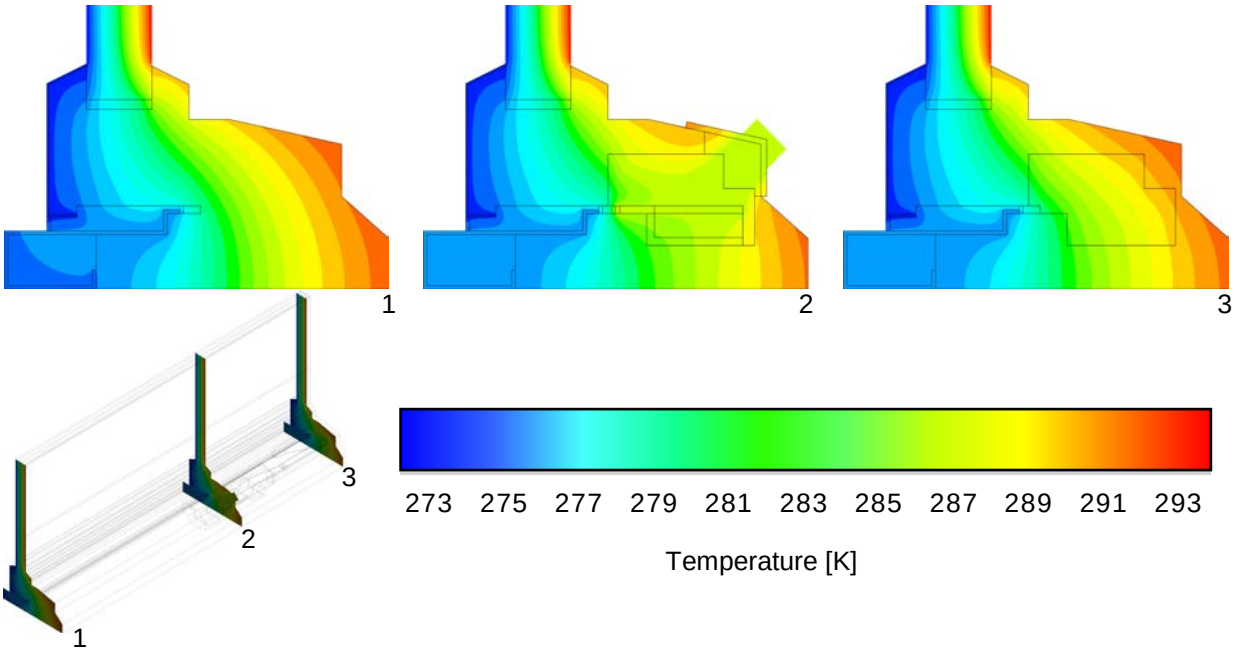

FIGURE 6. Temperature contours of Frame A at key frame cross-sections with (2 & 3) and without (1) hardware

Frame B

The hardware in Frame B results in a minor 1.3% increase in U-factor. The largest hardware piece, the operator, is located on the warm surface side external to the frame and has a relatively small impact on performance. All internal hardware is located in the large frame cavity area that spans from the warm side to the cold side interior frame surfaces. Figure 7 shows the simulated velocity vectors of this frame air cavity at key cross-sections of the frame. The contours show that the introduction of hardware (cross-sections 2 and 3) significantly reduces convection heat transfer to the warm side. The hardware is not continuous from the warm side to the cold side of the frame so the overall conduction through the frame cavity is nearly unchanged as is best shown in the isotherms of sections (1) and (3) of Figure 8. Since the convection and conduction through the cavity is relatively unchanged, the hardware has little impact on the overall thermal performance of the sill section.

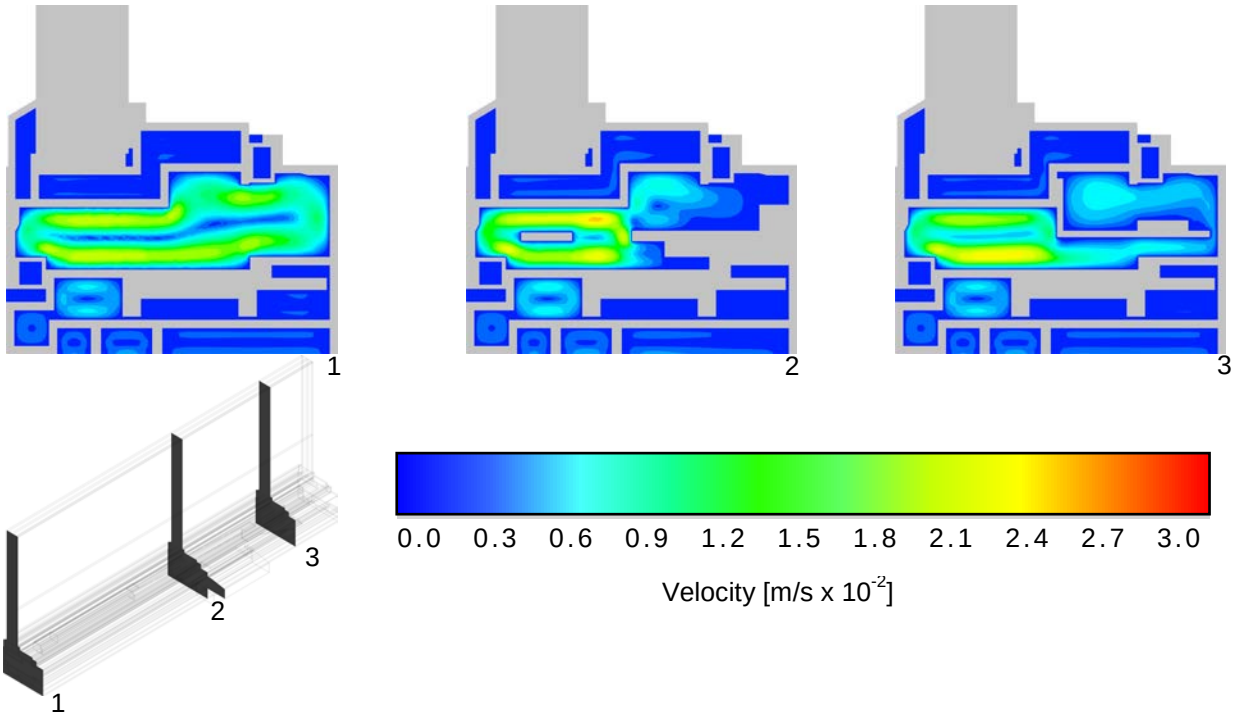

FIGURE 7. Velocity contours for the primary air cavity in Frame B with (2 & 3) and without (1) hardware

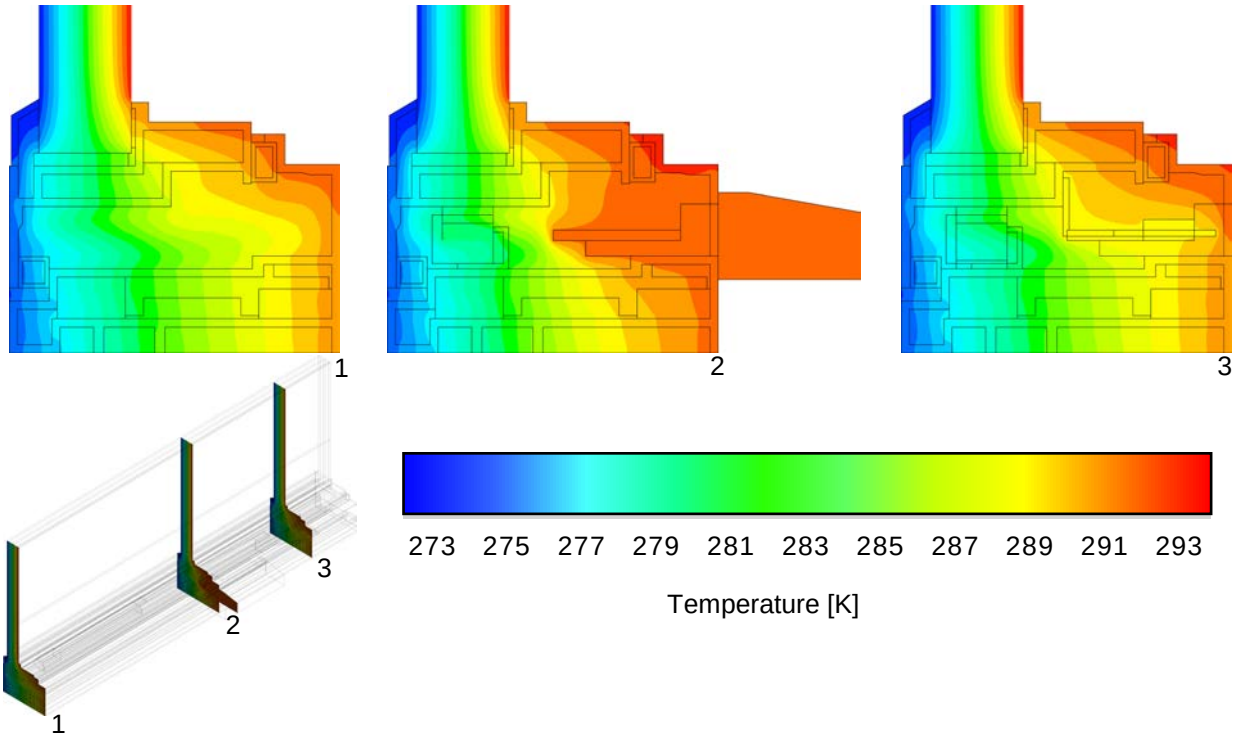

FIGURE 8. Temperature contours of Frame B at key frame cross-sections with (2 & 3) and without (1) hardware

Frame C

Frame C uses several frame cavity chambers inside a vinyl skeleton to construct a highly insulating frame. There is more hardware inside this frame than any other frame in the study. The significant amount of hardware requires numerous fastener penetrations through the vinyl skeleton, which compromises the cellular structure of the frame in the primary direction of heat transfer. Temperature contours of Frame C are shown in Figure 9. Section 3 is at a location with several hardware penetrations. Section 4 shows the reduced warm side and increased cold side temperatures within the cells of the frame when the highly conductive penetrations in the same cross-section are removed. The increased heat flux between the warm and cold sides of the frame can be clearly seen in Figure 10, which depicts the same cross-sections as 3 and 4 from Figure 9. The numerous penetrations, combined with the abundant hardware inside the frame results in a large 17.8% increase in U-factor when hardware is installed. When the frame is modeled with the same hardware, but without the penetrations as shown in cross-sections 3 and 4, the overall U-factor increases by only 1%. This demonstrates that compromising the cellular structure of this frame type is detrimental to its thermal performance.

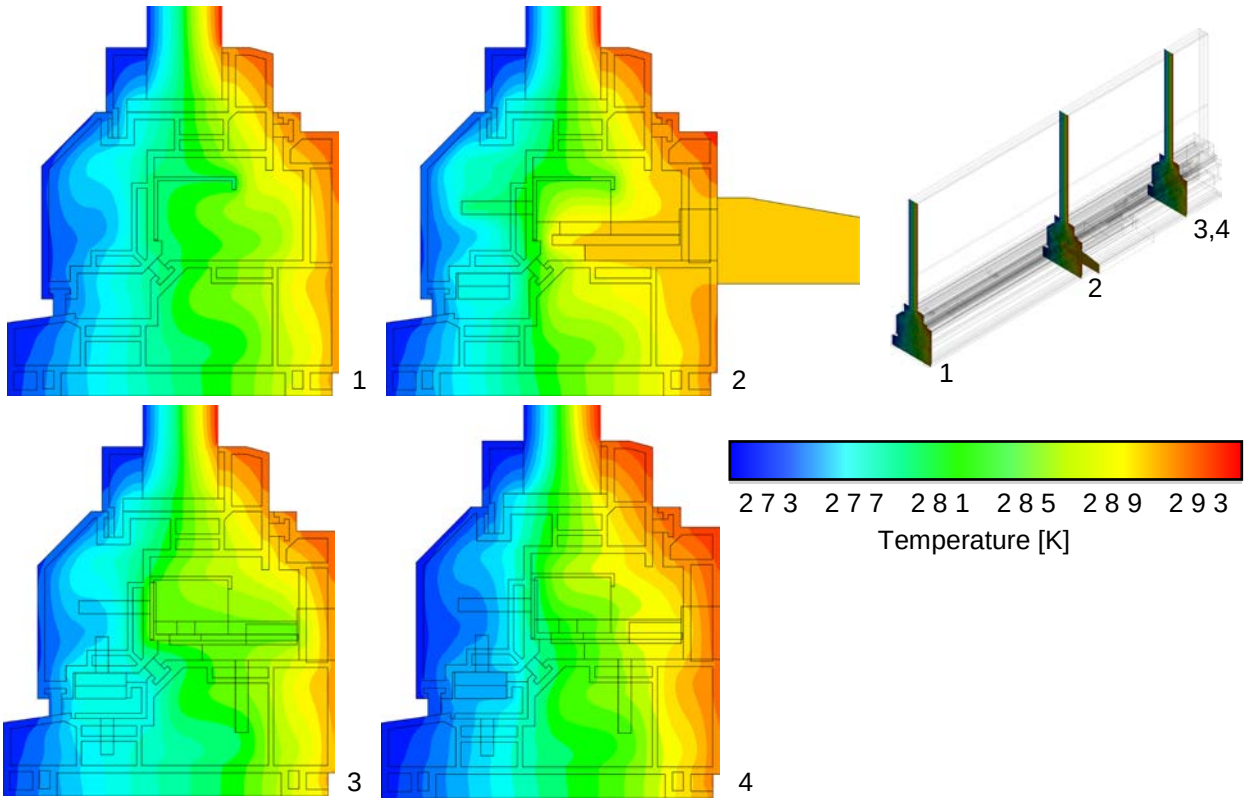

FIGURE 9. Temperature contours of Frame C at key frame cross-sections with (2 & 4) and without (1 & 3) hardware penetrations

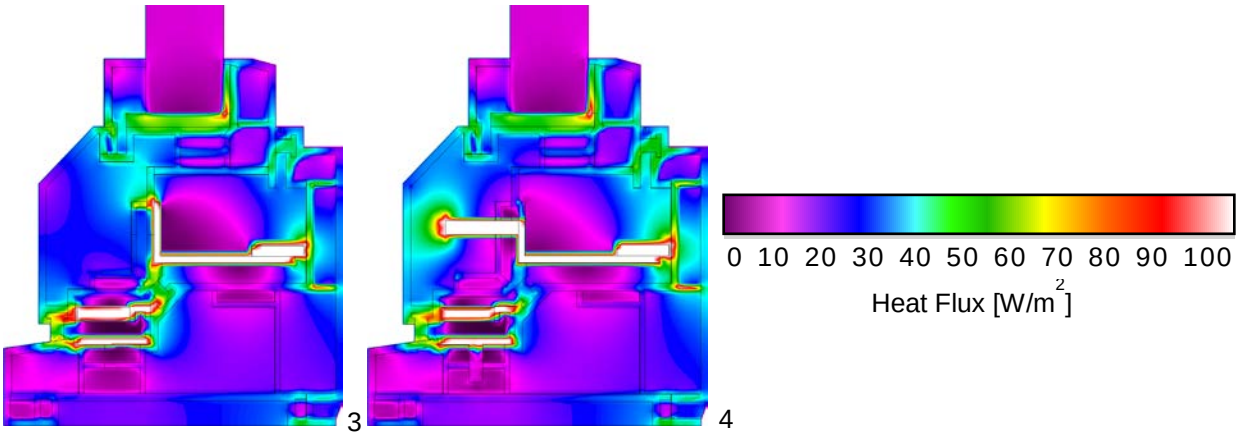

FIGURE 10. Heat flux contours of Frame C with (4) and without (3) hardware penetrations

Frame D

Frame D is the most highly insulating frame in this study and showed the least impact from hardware penetrations. This frame uses European style tilt-in hardware as opposed to the outward opening casement hardware used by the other frame types in this study. The hardware for this window type is constrained to the warm side of the frame, which minimizes the depth and effect of the hardware on thermal performance to a relatively small U-factor increase of 1.4%. The frame also implements highly insulating foam on the cold side which is uninterrupted by hardware. This provides a consistent cross-section of a highly insulating frame which is unmatched by Frames A-C. Figure 11 shows the isotherms of the frame at key cross-sections. Note that the hardware only has an impact on the frame's warm side surface temperature at cross-section 2.

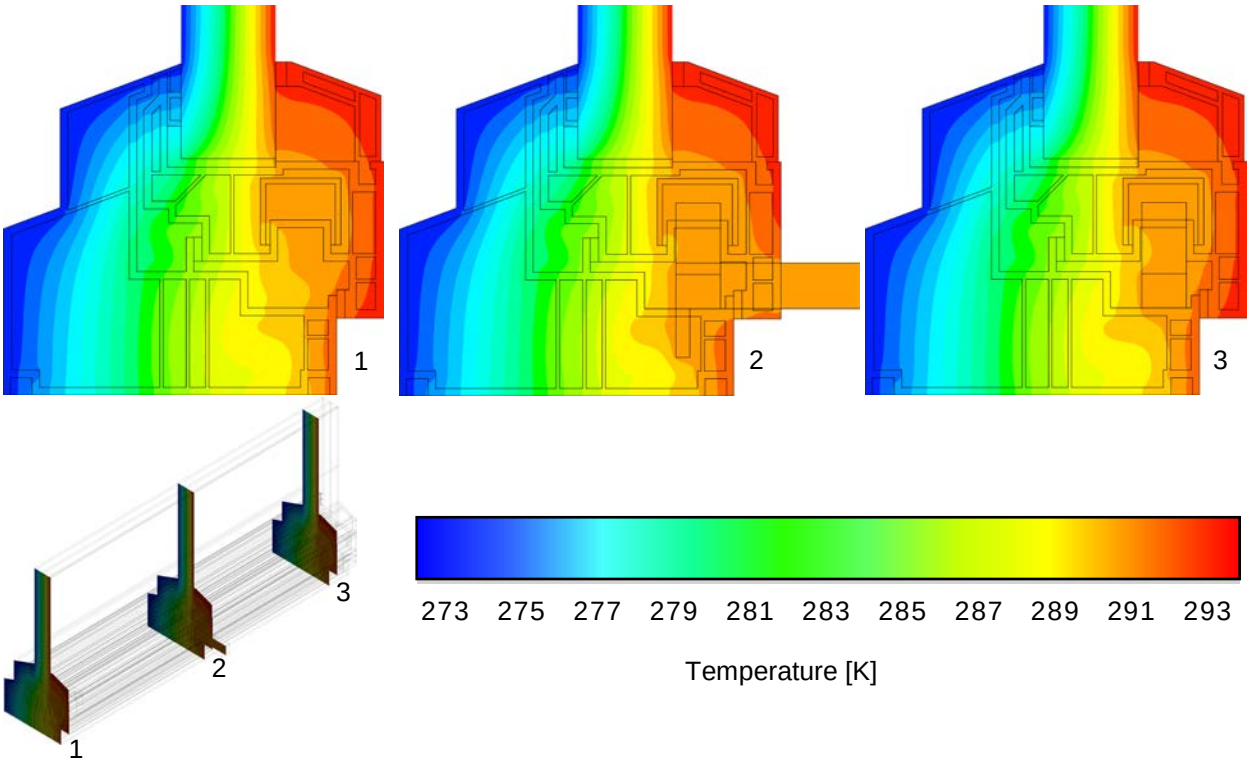

FIGURE 11. Temperature contours of Frame D at key frame cross-sections with (2 & 3) and without (1) hardware

CONCLUSIONS

Some conclusions can be drawn regarding the impacts of operating hardware on the thermal performance based on the individual frames, although few general trends can be observed due to the large design differences between each frame section modeled in this study. It is clear that the hardware used in typical out-opening casement windows may have a significant impact on the overall thermal performance of the frame, as two of the three frame sills modeled show reduced performance greater than 0.05 W/(m^2 K). It is also clear that the fastener types, operator location, and other factors related to the method of hardware implementation can significantly impact the effect of hardware on the frame. Greater penetration depth of hardware from the warm side surface to the cold side resulted in reduced thermal performance in three of the four frames modeled (Frames A, C, and D). In Frame B, the increased conduction of the hardware was nearly equalized by reduced convection heat transfer made possible by the hardware placement. Neither the base performance level nor the primary frame material appears to determine the thermal effect of hardware based on those metrics alone.

FUTURE WORK

The work presented in this study is the initial phase of a larger investigation to determine if the development of new modeling requirements for existing rating systems is needed to properly account for window hardware. This will include validating new

thermal rating methods and introducing new technical procedures for incorporating hardware effects into whole window thermal rating methods.

Based on the results from this initial study, we will perform more detailed sensitivity analysis on frame materials, hardware locations, and hardware penetrations. We will also extend our investigations to the performance impacts for alternative frame profiles, including jambs and heads, and frame types, including vertical and horizontal sliders and patio doors. A sensitivity analysis of full frame thermal performance impacts with the same frames is also planned to determine the impact of hardware when the glazing systems improves without changes to the frame. Experimental validation testing of select products in a guarded hot box to verify performance impacts demonstrated in the modeling is also under consideration.

ACKNOWLEDGEMENTS

This work was supported by the Assistant Secretary for Energy Efficiency and Renewable Energy, Office of Building Technology, Building Technologies Program of the U.S. Department of Energy under Contract No. DE-AC02-05CH11231, and the Research Council of Norway, Lian Trevarefabrikk and Lawrence Berkeley National Laboratory (LBNL) through the NTNU and SINTEF research project "*Improved Window Technologies for Energy Efficient Buildings*" (EffWin).

REFERENCES

Gustavsen, A., H. Goudey, S. Uvsløkk, G. Talev, D. Arasteh, C. Kohler, and B.P. Jelle. 2010. Experimental Examination of the Thermal Transmittance of High Performance Window Frames and Comparison with Numerical Simulations. Proceedings of the Thermal Performance of the Exterior Envelopes of Whole Buildings XI International Conference, December 5-9, 2010. Clearwater Beach, Florida.

Gustavsen, A., B.T. Griffith, D. and D. Arasteh. 2001. Three-Dimensional Conjugate Computational Fluid Dynamics Simulations of Internal Window Frame Cavities Validated Using Infrared Thermography. ASHRAE Transactions. Vol. 107(2), pp. 538-549.

Gustavsen, A., B. P. Jelle, D. Arasteh and C. Kohler. 2007. State-of-the-Art Highly Insulating Window Frames – Research and Market Review. Project report 6, SINTEF Building and Infrastructure.

Gustavsen, A., S. Grynning, D. Arasteh, B.P. Jelle, and H. Goudey. 2011. Key Elements of and Materials Performance Targets for Highly Insulating Window Frames. Energy and Buildings, Volume 43(10).

International Organization for Standardization. 2003. ISO 10077-2. Thermal performance of windows, doors and shutters—Calculation of thermal transmittance, Part 2: Numerical method for frames.

Jelle, B.P., A. Hynd, A. Gustavsen, D. Arasteh, H. Goudey and R. Hart. 2012. Fenestration of Today and Tomorrow: A State-of-the-Art Review and Future Research Opportunities. Solar Energy Materials and Solar Cells, Volume 96, pp. 1-28.

National Fenestration Rating Council. 2010. NFRC-100-2010E0A1. Procedure for Determining Fenestration Product U-factors.

National Fenestration Rating Council. 2010. NFRC-101-2010E2A7. Procedure for Determining Thermophysical Properties of Materials For Use in NFRC-Approved Software Programs.

Zhao, Y. 1998. Investigation of heat transfer performance in fenestration system based on finite element methods. Ph.D. dissertation. Massachusetts: Department of Mechanical and Industrial Engineering, University of Massachusetts, Amherst.